*Kodathalapalli Sudheer, et. al. International Journal of Engineering Research and Applications*
*www.ijera.com*
*ISSN: 2248-9622, Vol. 12, Issue 3, (Series-II) March 2022, pp. 05-19*

RESEARCH ARTICLE OPEN ACCESS

# To predict mechanical properties of XLPE insulation cables under thermal ageing using neural networks and fuzzy logic techniques

Kodathalapalli Sudheer[1], Dr.V.Veeranna[2]
[1]*Research Scholar, Dept of Mechanical Engineering, Rayalaseema University, Kurnool, Andhra Pradesh, India*
[2] *Principal, Dept of Mechanical Engineering, St.Johns College of Engineering Technology, Yemmiganur, Andhra Pradesh, India*

**ABSTRACT**
The widespread use of cross-linked poly- ethylene (XLPE) as insulation within the manufacturing of medium and high-voltage cables could even be attributed to its outstanding mechanical and electrical properties. However, it's well-known that degradation under service conditions is that the key problem within the utilization of XLPE as cable insulation. Laboratory testing of aging insulation is time consuming and inexpensive. To avoid such costs, we've got developed two models which are supported artificial neural networks (ANNs) and logical system (FL) to predict the insulation properties under thermal aging. The proposed ANN can be a supervised one supported radial basis function Gaussian and trained by random optimization method algorithm. The FL model relies on the utilization of fuzzy inference system. Both models are accustomed predict the mechanical properties of thermally aged XLPE. The obtained results are evaluated and compared to the experimental data comprehensive by using many statistical parameters. it's concluded that both models give practically the identical prediction quality particularly, they need ability to breed the nonlinear behavior of the insulation properties under thermal aging within acceptable error. Furthermore, our ANN and FL models are utilized within the generalization phase where the prediction of the long run state (not reached experimentally) of the insulation is created possible. Additionally, costs and time is reduced.

**Keywords** XLPE insulation. Neural network .Fuzzy logic

---

Date of Submission: 10-03-2022 Date of Acceptance: 26-03-2022

---

## I. INTRODUCTION

Electric cables are important elements which make sure the transmission of power. In such cables, polymer materials provide electrical insulation [1].]. Compared to some varieties of polymers like vinyl polymer (PVC), ethylene-propylene copolymer (EPR) and ethylene-acetate copolymer (EVA) which are of common use for such purpose, the polyethylene (PE) in its cross-linked form (XLPE) is incredibly recommended [2]. This material is widely employed in medium-voltage (MV) and high- voltage (HV) cables up to 500 kV [3] because it's excellent dielectric strength and electrical resistivity, similarly as of its excellent physical properties including resistance to cracking and moisture penetration [4]. Many factors can cause the cable failure. Among others, one can quote: presence of voids and impurities within the material, incorrect handling during installation, inappropriate mechanical and electrical use and aging of polymeric insulation under service conditions. This latter presents the foremost important explanation for the cable failure [1]. Under operating conditions, cables are permanently exposed to electrical, thermal, mechanical, and environmental loads [5]. When exposed to heat, thermal degradation occurs, causing irreversible damage to the cable insulation. Under heat conditions, thermal aging occurs and causes an irreversible damage of the cable insulation. Under temperature stress and over a period of your time, chemical composition [6] and physical morphology [7, 8] of XLPE may change. Consequently, several properties may alter. for instance, volume resistivity reduces, dielectric losses increase [9] and mechanical properties decrease [10]. The great importance of XLPE as insulation motivates researchers in laboratories worldwide to research many experimental techniques so on induce more insight on the state of the insulation. the knowledge derived from this overall work helps to know the degradation mechanisms of the fabric under service conditions. On the opposite hand, these investigations are focused on the XLPE insulation

morphological structure to understand whether this material is possibly reused [11]. Many recent experimental studies have attempted to diagnose the electrical tree of XLPE cables [12-15].The effect of partial discharges on the electrical properties of the cable has been studied during a really lot of investigations [16, 17]. Much work has been disbursed, and thus the chemical modifications generated by aging and its consequences on the mechanical and electrical properties of XLPE [10, 18] were analyzed. All these investigations are cost-effective and time-consuming. It can take a few years to build up a large enough database to address energy-related economic problems and perform simple maintenance. As a result, efforts have been undertaken to simulate the trend.. Newest techniques are based on the use of intelligent systems. These innovative methodologies assist scientists, researchers, and engineers in making efficient use of the database and determining the future condition of the insulation system under ageing with greater precision and in less time. Different modelling and prediction methods based on artificial neural networks (ANNs) and fuzzy logic (FL) systems have grown in popularity over the last two decades, and many academics have employed them for a variety of engineering applications [22–25]. In electrical engineering, especially in high-voltage field, a lot of applications of ANN can be found [26–30].Chen et al. studied partial discharge pattern identification in high-voltage power apparatus investigated a novel extension neural network method. Mohanty and Ghosh [27]. used a multilayer feed-forward network and a radial basis function network to forecast the breakdown voltage due to PD in cavities for various insulating materials. Teguar et al. [28] and Genc¸og˘lu and Cebeci [29] investigated two types of neural networks (RBFG and MLP) to predict the flashover of polluted high-voltage insulators. Mohanty used a multilayer feed-forward network and a radial basis function network to forecast the breakdown voltage due to PD in cavities for various insulating materials. The intent of this paper is to apply the fuzzy logic approach to predict, under thermal aging, the mechanical properties of XLPE insulation used in medium- and high- voltage cables. The results of this strategy will be compared to the supervised neural network that will be used. The latter is trained using the random optimization technique (ROM) algorithm and is based on radial basis function Gaussian (RBFG). We believe that the use of fuzzy logic theory to the prediction of high-voltage cables is novel and of considerable relevance in the creation of industrial instruments

## II. EXPERIMENTAL STUDY

### 2.1 Material

All tests were conducted using commercial XLPE UNION CARBIDE 4201, which is often used as a medium-voltage cable insulation. This material, in its granule form, contains polyethylene blended with 2 % of dicumyl per- oxide (DCP) as cross-linking agent and 0.2 % of IRGA- NOX 1035 as an antioxidant. Two coaxial cylindrical semiconducting screens are extruded simultaneously during manufacture to cover the XLPE insulation, resulting in a three-layer system. 2.2 Thermal aging experiments The polyethylene is granulating with its various additions. These granules were moulded into 2 mm thick plates using a press machine that was heated to 180°C and pressed at 300 bars. The plates were then According to the IEC 540 (International Electrotechnic Committee) document, cut into dumbbell-shaped samples with a length of 7.5 cm. According to the IEC 216 publication, these samples were aged at four different temperatures. Two temperatures are situated below the melting temperature of XLPE which are 80 and 100 °C. Two more (120 and 140 °C) are located above the polymer's melting point. For the first two temperatures, the age time is 5000 hours; for 120 and 140 °C, the ageing time is 3500 hours and 2000 hours, respectively. The ageing procedure was carried out in an oven with forced air circulation. Maintain a temperature of 2 °C for the samples on average. Ten samples were taken after each 500-hour age period and then subjected to tensile stress. The studies entail breaking the sample at room temperature with a dynamometer moving at a speed of 50 mm/min. At the same time, elongation at rupture and tensile strength were measured.

## III. INTELLIGENT PREDICTION METHODS

### 3.1 Artificial neural network (ANN) model

In addition to its ability of classification and diagnosis, ANN can be used in function estimation branch [29].Variations in XLPE mechanical properties can be thought of as nonlinear functions in this scenario, and hence can be approximated with ANN models. We employed a feed-forward neural network to forecast the mechanical properties of XLPE insulating cables under thermal ageing. The radial basis function is used to build this network (RBF). Only the outline of the employed RBF neural network will be shown in the following sections. Further detail can be found in [34, 35]. The input layer, the hidden layer, and the output layer are the three layers of the RBF neural network utilised here (Fig. 1). The input layer is made up of n neurons that correspond to the experimental values of the XLPE attribute in

question. These n values, which differ from one ageing temperature to the next, were utilised to train the network. In the case of ageing at 80°C, the number of n is 5, while in the case of ageing at 120°C, the value is 3 or 4 (depending on the specified attribute). One neuron corresponds to the next projected value in the output layer. 6 of the property (pn?1).1) To eliminate the problem of local minima that can occur when using the back-propagation approach, we used the random optimization method (ROM) to train the network (BPA). The flowchart of the ROM training algorithm is shown in Figure 2.. The Gaussian function represented in Eq. (1) [36] is used as the activation function.

$$\rho_j(x_i) = \exp\left(-\frac{1}{2}\sum_{i=1}^{n}\frac{(x_i - c_{ij})^2}{\sigma_{ij}^2}\right)$$

Where $C_{ij}$ i = 1, n and j = 1, m are the RBFG centers, $X_{ij}$ define the width of Gaussians.

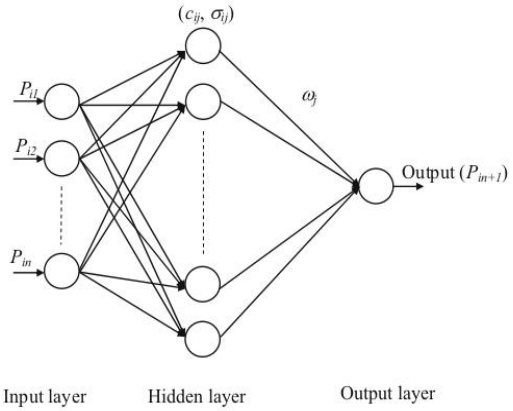


output value is given by Eq. (2).

$$y^* = \left(\sum_{j=1}^{m} w_j \rho_j(x_i)\right) \Big/ \left(\sum_{j=1}^{m} \rho_j(x_i)\right)$$

The many prediction phases are depicted in Fig. 3's flowchart, and more information is available in our earlier work [34, 37].The proposed modeling procedure is carried out with the help of 54 sets of experimental input–output patterns which illustrate the various values of various attributes as a function of ageing time and two ageing temperatures. Only 26 of the 54 sets are utilised to train the proposed ANN model, with the remaining 28 sets being used for testing. The 26 training sets utilised were chosen to represent all of the first findings achieved under thermal ageing and for each property. The top 5 values obtained between 0 and 2000 h with ageing step duration of 500 h are used as training sets in the case of elongation at rupture at 80 °C. The testing is done with the 6 most recent values, which are between 2000 and 5000 hours old.. The same procedure is carried out with the other properties and other aging conditions.

**3.2 Fuzzy logic model**

It is well known that the pioneer of fuzzy logic (FL) was Zadeh in 1965 [38]. This study use the developed fuzzy theory to forecast the mechanical parameters of XLPE high-voltage insulation cables, namely tensile strength (P1), elongation at rupture (P2 ) and Hot Set Test (P3 ) as a function of aging time (t) and aging temperature (T), that is P i = f(t, T). A Mamdani fuzzy inference The FIS system was chosen and constructed using 28 sets of the same 54 trial sets used in the ANN model. The developed FIS's main scheme is shown in Fig. 4, and further information and descriptions of its many components may be found in [30–32].The chosen input/output membership functions are presented in Fig. 5.With nine partitions matching to nine linguistic qualities, they have a hybrid shape (trapezoidal and triangular). The temperature fluctuates in a discrete manner and takes several values during the structure identification process. In our scenario, the input variable is not defuzzified. The carried-out experimental ageing is done at four temperatures, as reported in Sect. 2.2, however for the sake of brevity, only two temperatures will be considered in the prediction phase. These two temperatures are 80 °C, which is below XLPE's melting temperature (about 105 °C), and 120 °C, which is over the polymer's melting peak. The set of linguistic values assigned to t and P ii = 1, 3 is given by Eq. (3).

r = {Small (SS), Small-Medium(SM), Small-Large (SL) Þ; Medium-Small, Medium-Medium (MM), Medium-Large (ML), Large-Small (LS), Large-Medium (LM), Large-Large (LL)} (3)

Tables 1, 2 and 3 show the link between the verbal values and the actual values for t and Pi I = 1, 3. For t and Pi I = 1, 3, the membership functions (MFs) are t and pi, respectively. The rule base can be developed with a maximum of 27 rules from the empirically generated data for each temperature since t and each of the characteristics can have nine linguistic values (Table 4). The AND operator was used to connect fuzzy variables in the rule base, and the "max–min" decomposition technique was used to associate rules. Also $\mu_t$ and $\mu_{pi}$ would be having nine components corresponding to each linguistic value as:

$$\mu_t = \{\mu_{tSS}, \mu_{tSM}, \mu_{tSL}, \mu_{tMS}, \mu_{tMM}\ \mu_{tML}\ \mu_{tLS}\ \mu_{tLM}, \mu_{tLL}\} \quad (4)$$

$$\mu_{pi} = \{\mu_{PiSS}, \mu_{PSM}, \mu_{PiSL}, \mu_{PiMS}, \mu_{PiMM}, \mu_{PiML}, \mu_{PiLS}, \mu_{PiLM}, \mu_{PiLL}\} \quad (5)$$

The following equation can be used to express the previous membership functions mathematically:

$$\mu_x = \begin{cases} 1 & x<a \\ b\text{-}x)/(b\text{-}a) & a<x<b \\ (x\text{-}b)/(c\text{-}b) & b<x<c \\ (d\text{-}x)/(d\text{-}c) & c<x<d \\ (x\text{-}d)/(e\text{-}d) & d<x<e \\ 1 & x>e \end{cases} \quad (6)$$

As for computation, the input and output variables are introduced in the MATLAB® environment and the fuzzy toolbox was used to establish these variables as shown in Fig. 6. Each input variable and output variable were fuzzified with membership function graphically designed with toolbox.

## IV. RESULTS AND DISCUSSION

### 4.1 Analysis of experimental results

The goal of this research is to build a neural network and fuzzy logic model using experimental ageing data.

As a result, the experimental data have been scrutinized.

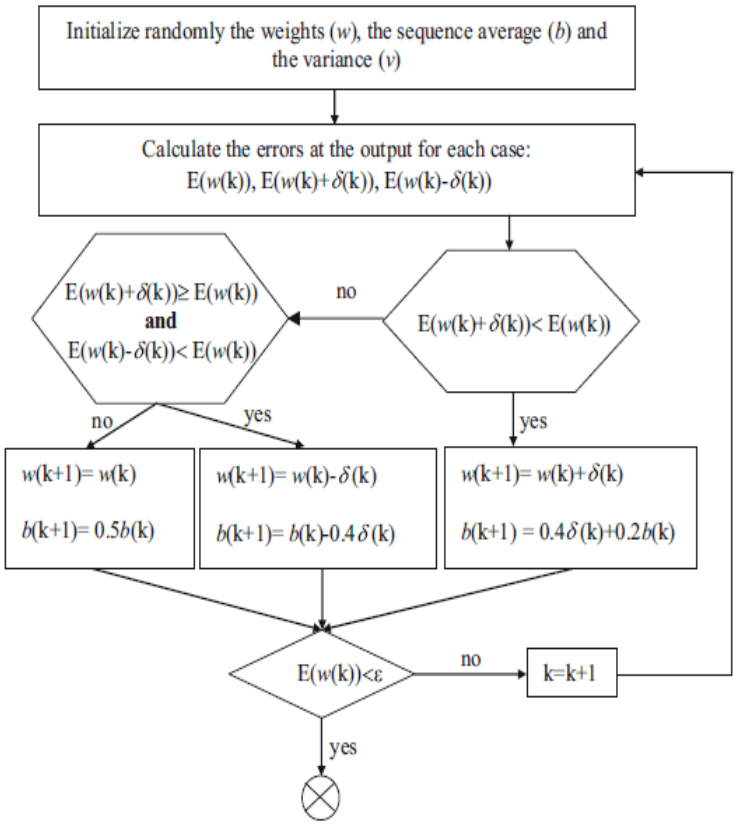


**Fig. 2** Training algorithm of ROM

**Fig. 3** Flowchart for prediction with RBFG neural network

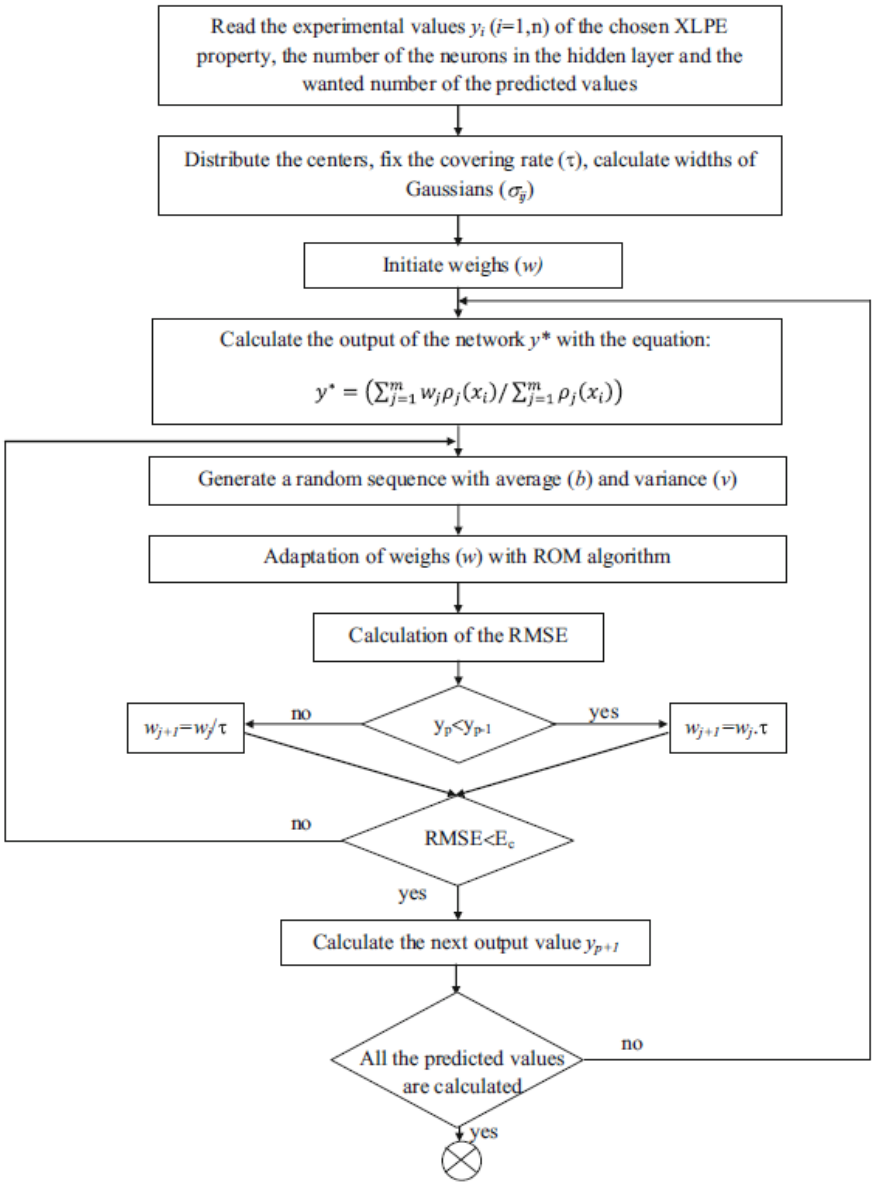


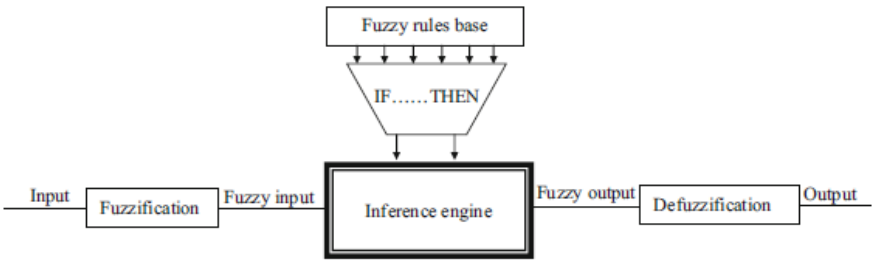


**Fig. 4** A fuzzy inference system

Fig. 5 Input/output system μ variable membership functions

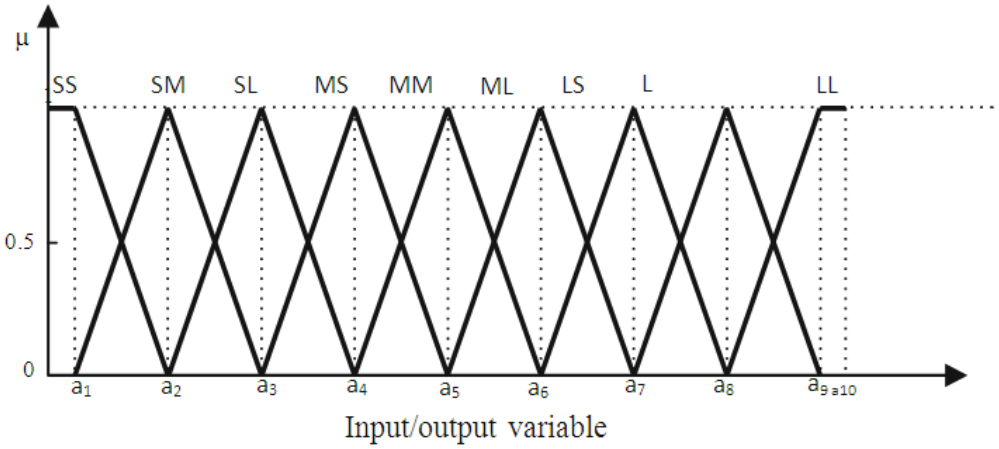


The association between linguistic values and true ageing time t values is shown in **Table 1**

| Linguistic values | Temperature ageing time (h) a temperature of 80 degrees Celsius | Temperature ageing time (h) 120 degrees Celsius |
|---|---|---|
| Small Small | 0–1250 | 0-1000 |
| Small Medium | 750–1750 | 666.66 –1333.33 |
| Small Large | 1250–2250 | 1000–1666.66 |
| Medium Small | 1750–2750 | 1333.33–2000 |
| Medium Medium | 2250–3250 | 1666.66–2333.33 |
| Medium Large | 2750–3750 | 2000–2666.66 |
| Large Small | 3250–4250 | 2333.33–3000 |
| Large Medium | 3750–4750 | 2666.66–3333.33 |
| Large Large | 4250–5000 | 3000–3500 |

At 80 degrees Celsius, **Table 2** shows the link between linguistic values and real values for a variety of variables

| Linguistic values | Tensile resistance (P1) | Rupture elongation (P2) | Hot Set Test (P3) |
|---|---|---|---|
| Small Small | 16.42–17.38 | 510–513 | 75–105.83 |
| Small Medium | 16.725–17.96 | 510.5–515.25 | 101.44–109.72 |
| Small Large | 17.38–18.315 | 513.5–520.25 | 105.83–113.61 |
| Medium Small | 17.96–18.47 | 515.25–530 | 109.72–117.5 |
| Medium Medium | 18.315–18.625 | 520.25–540.93 | 113.61–121.39 |
| Medium Large | 18.47–18.85 | 530–551.93 | 117.5–125.28 |
| Large Small | 18.625–19.005 | 540.93–562.875 | 121.39–129.17 |
| Large Medium | 18.85–19.355 | 551.93–568.75 | 125.28–133.06 |
| Large Large | 19.005–21.64 | 568.75–606.25 | 129.17–135 |

**Table 3** shows the relationship between linguistic and real values at 120 degrees Celsius for a variety of qualities

| Linguistic values | Tensile resistance (P1) | Rupture elongationP2) | Hot Set Test (P3) |
|---|---|---|---|
| Small Small | 9.87–13.69 | 250–394.99 | 80–132.5 |
| Small Medium | 11.14–16.24 | 298.33–491.66 | 127.5–137.5 |
| Small Large | 13.69–17.64 | 394.99–542.56 | 132.5–140.83 |
| Medium Small | 16.24–17.88 | 491.66–547.69 | 137.5–142.49 |
| Medium Medium | 17.64–18.12 | 542.56–552.83 | 140.83–144.16 |
| Medium Large | 17.88–18.41 | 547.69–557 | 142.49–150 |
| Large Small | 18.12–18.73 | 552.83–560.2 | 144.16–160 |
| Large Medium | 18.41–19.06 | 557–563.4 | 150–170 |
| Large Large | 18.73–21.64 | 560.2–606.25 | 160–175 |

**Table 4** Rule base of proposed fuzzy logic model

| Temperature | Input Time *t* | Output Mechanical properties | | |
|---|---|---|---|---|
| | | $P_1$ | $P_2$ | $P_3$ |
| 80 °C | SS | LL | LL | SS |
| | SM | LM | LL | SM |
| | SL | LS | LS | SL |
| | MS | ML | ML | MS |
| | MM | MM | MM | MS |
| | ML | MS | MS | ML |
| | LS | SL | SL | ML |
| | LM | SM | SM | ML |
| | LL | SS | SS | LS |
| 120 °C | SS | LL | LL | SS |
| | SM | LM | LM | SM |
| | SL | LS | LS | SL |
| | MS | ML | ML | MS |
| | MM | MM | MM | MM |
| | ML | MS | MS | ML |
| | LS | SL | SL | LS |
| | LM | SM | SM | LM |
| | LL | SS | SS | LL |

and discussed in this paper briefly. For brevity reasons, only results for aging temperatures 80 and 120 $^{o}$C will be presented in this section. The same behavior has been observed in the case of 100 and 140 $^{o}$C and can be analyzed in a similar way as 80 and 120 $^{0}$ C. In Figs. 7a, b and 8a, b, the mean values of mechanical parameters (tensile strength and elongation at rupture) are displayed as a function of ageing time. The findings of a series of experiments revealed that the mechanical properties of XLPE deteriorate with ageing time This diminution is slight at temperature of 80 $^{0}$C. We observed an abrupt drop in the examined properties at elevated temperatures (above the melting point of XLPE). The elongation at rupture decreases from 600 to 250 % and the tensile strength decrease from 22 to 10 N/mm$^2$ after 3500 h of aging at 120 $^{o}$C

The diminution of mechanical characteristics is attributed to the thermal-oxidant degradation of the material which is followed by chains scission[39,40] The chain scissions result in a reduction in molecular mass and cross-linking rate, resulting in material fragility. Chain scission reactions, on the other hand, contribute to the creation of vinylidene and vinyl groups, as well as other unsaturated groups, on the XLPE structure. The colour changes of the material during thermal stress are mostly caused by these groups In general, morphological characteristics such as crystallinity degree, crystallite thickness, and crystalline-amorphous ratio control mechanical properties [41]. Mechanical characteristics and crystallinity degree vary in a comparable fashion with thermal ageing, according to Andjelkavic and Rajakovic [42], implying that there is some correlation .Thermal degradation of cross-linked polyethylene has been

**Fig .6** Interface of implemented FIS System with fuzzy toolbox

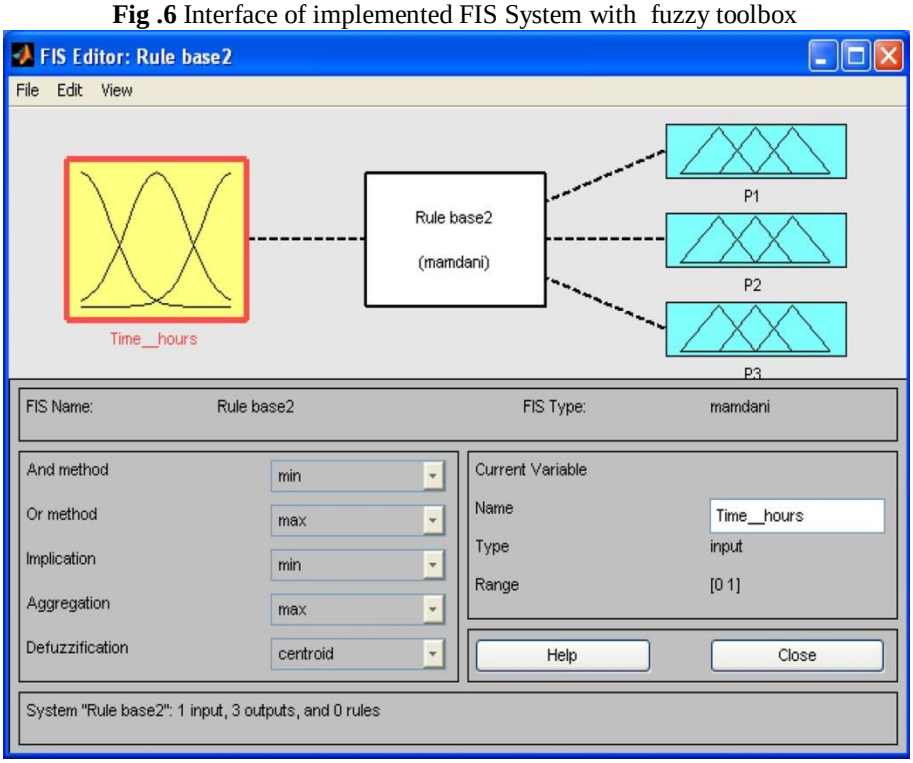


**Fig. 7** Experimental and predicted values of tensile strength: **a** 80 °C and **b** 120 °C

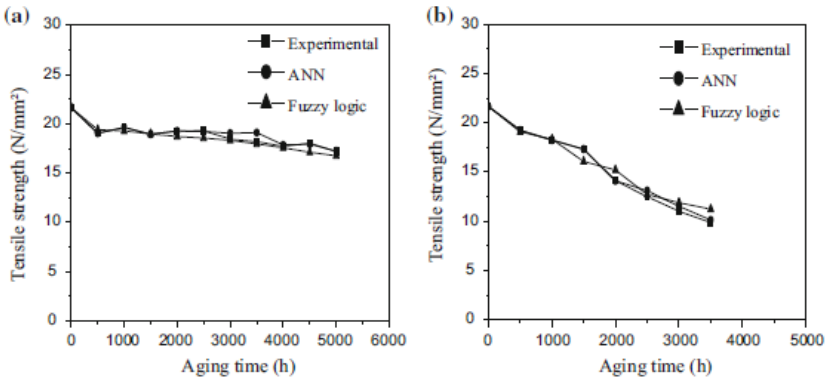


**Fig. 8** Experimental and predicted values of elongation at rupture: **a** 80 °C and **b** 120 °C

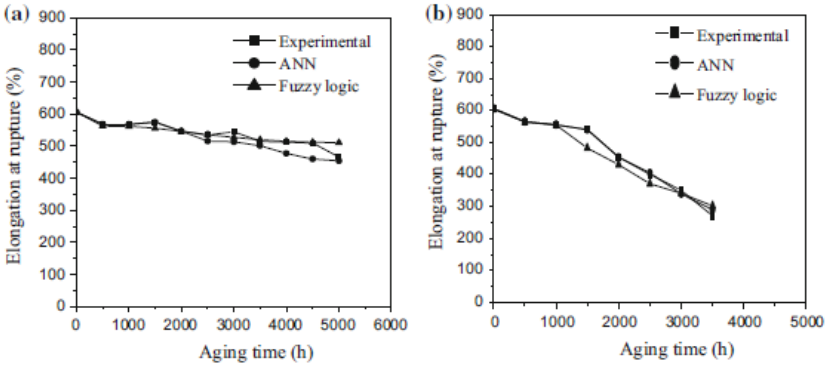

attributed to an antioxidant loss. The degradation pathways are inhibited by this additional ingredient. Volatile compounds are produced in tiny vacuoles during the cross-linking process. A portion of the trapped gases (hydrocarbons, ketones, alcohols) can be released and replaced by water or oxygen during thermal ageing, which is the primary cause of degradation.

We conducted a series of tests to assess the Hot Set Test (HST) elongation to investigate the evolution of XLPE cross-linking degree. The HST was measured on dumbbell-shaped samples held vertically in a vented oven regulated at 200 °C and subjected to 0.2MPa stress in the oven, as defined in the IEC 540.The obtained results for 80 and 120 °C are displayed in Fig. 9 a, b. At heat deformation, a maximum of cross-linking density corresponds to a minimum of elongation [43]. According to the ageing time, the cross-linking degree drops at three different speeds for all ageing temperatures. At the start of the ageing process, the elongation grows quickly in the first stage. The second phase is characterized by a weak increase in the elongation; there- fore, thermal aging does not have practically any effect on the degree of cross-linking During the third, elongation develops rapidly, particularly at temperatures above the material's melting point, resulting in a rapid fall in cross-linking degree.

**4.2 Prediction results analysis**

In this study, we have used artificial neural networks trained by ROM and fuzzy logic to predict mechanical properties of XLPE insulation cables under thermal aging Simulations were run multiple times with various parameters changed, and the results of the best decision are shown for each approach. After a series of simulations with various learning times, the ANN's learning time was chosen. The chosen learning period should provide the highest possible learning quality. We trained the network for a learning time less than the maximum ageing period for each temperature by using a 500-hour learning step. The neural network then forecasts each property for the duration of the experiment. This procedure allows us to validate the prediction quality of the network. We employed a 2000-hour learning time to train for an ageing temperature of 80 °C.

Fig. 9 Experimental and predicted values of Hot SetTest: a) 80 °C and b) 120 °C

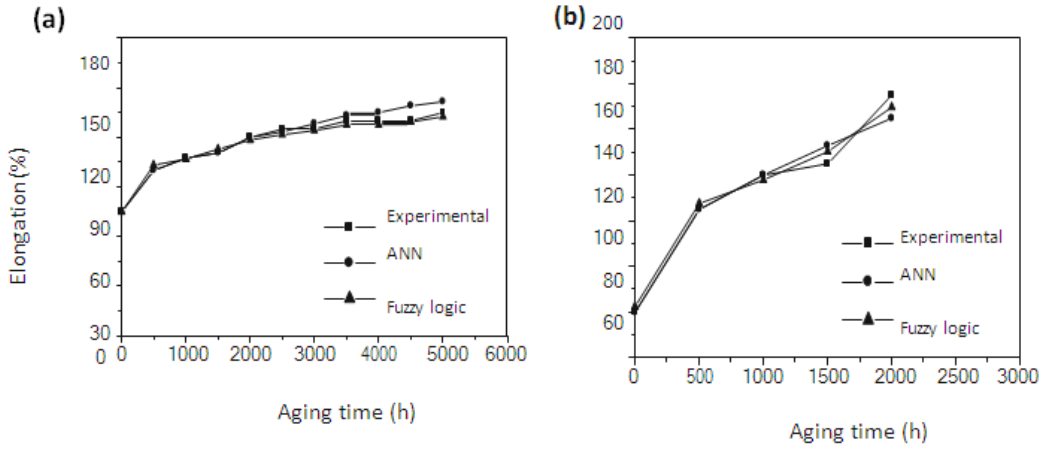


all properties we employed a learning time of 1500 hours to train elongation at rupture and tensile strength at 120 degrees Celsius, and 1000 hours to train the Hot Set Test. All of these learning periods produce the best prediction outcomes. The variance of the RMS error for the training data as a function of the number of repetitions, as shown in Fig.10, is considered when deciding on the evaluation criterion. As expected, the RMS error decreases steadily as training advances until stabilizing. Therefore, training should be stopped at the value where RMS error does not change much with number of iterations to consider the least training timeof the network.

Figures 7a, b, 8a, b, and 9a, b show both experimental and anticipated results using ANN and FL models. Figure 7a, b shows the experimental and projected tensile strength values for temperatures of 80 and 120 degrees Celsius. Figures 8a, b and 9a, b, respectively, show experimental and projected values for elongation at rupture and the Hot Set Test. All of these graphs show that the expected and experimental findings are similar. To make this result more obvious, we must use statistical analysis to quantify the comparison.

*4.2.1 Analytical statistics*

To make statistical analysis useful, three factors must be considered. To begin, we must compare the projected values for each property obtained with each model to the experimental

findings. Each model's prediction accuracy is estimated using a 1:1 line, which represents 100 percent accuracy. The root mean square error (RMSE), mean absolute relative error (MARE), determination coefficient ($R^2$) calculated using the least mean square approach, and the index of agreement d are employed as evaluation criteria in the second stage. Finally, each example is compared using the Bland–Altmanplot.

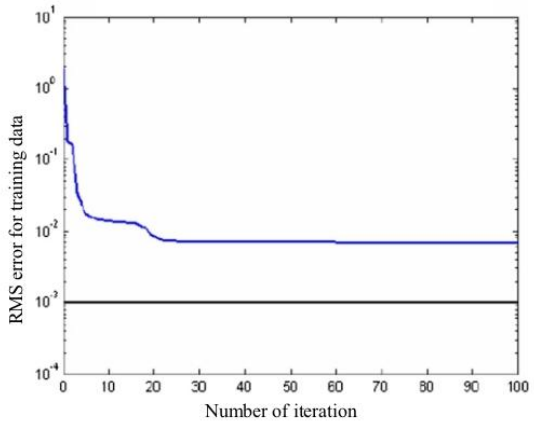


**Fig. 10** Variation of RMS error for the training data with the number of iterations

The plot of a 1:1 line that includes both experimental and anticipated values derived by ANN and FL, Figures 11a, b, 12a, b, and 13a, b show the tensile strength, elongation at rupture, and Hot Set Test models, respectively. These diagrams also show the linear least square fit line, its equation, and the $R^2$ values.

The $R^2$ and d coefficients are used to calculate the degree of linearity between two variables. Willmot [44] introduced the index of agreement to address $R^2$'s insensitivity to differences unmeasured and anticipated means and variances. The range of d is similar to that of $R^2$, and it ranges from 0 (no correlation) to 1 (strong correlation) (perfect fit). The variables $R^2$ and d are defined as follows:

**Fig. 11** Linear fit of experimental and predicted values of tensile strength: **a** 80 °C and **b** 120 °C

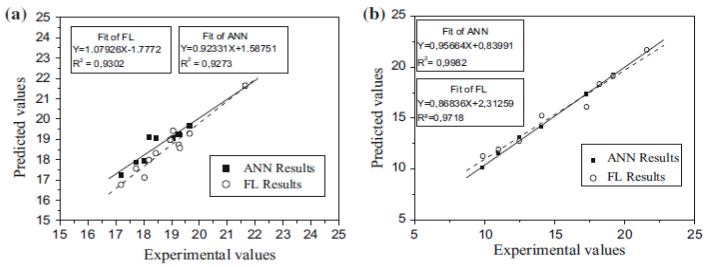


**Fig. 12** Linear fit of experimental and predicted values of elongation at rupture: **a** 80 °C and **b** 120 °C

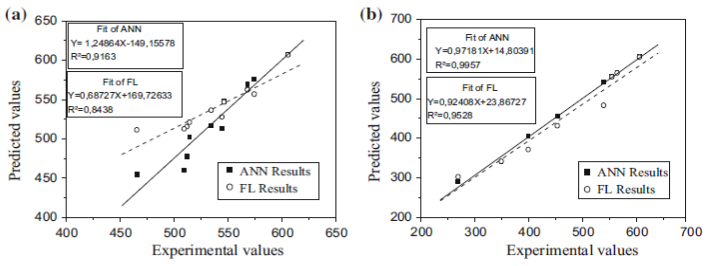


**Fig. 13** Linear fit of experimental and predicted values of Hot Set Test: **a** 80 °C and **b** 120 °C

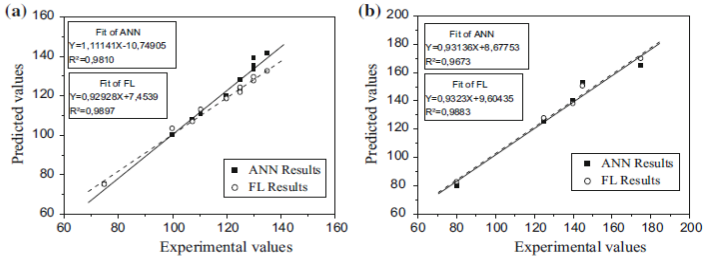

$$R^2 = \frac{\left(n\sum_{i=1}^{n} T_i P_i - \sum_{i=1}^{n} T_i \sum_{i=1}^{n} P_i\right)^2}{\left(n\sum_{i=1}^{n} T_i^2 - \left(\sum_{i=1}^{n} T_i\right)^2\right)\left(n\sum_{i=1}^{n} P_i^2 - \left(\sum_{i=1}^{n} P_i\right)^2\right)} \quad (7)$$

$$d = 1 - \frac{\sum_{i=1}^{n} [P_i - T_i]^2}{\sum_{i=1}^{n} \left(|P_i - \overline{T}| + |T_i - \overline{T}|\right)^2} \quad (8)$$

where $P_i$ is the predicted value of property by the chosen model, $T_i$ is the target value (measured value of the property), and $\overline{T}$ is the average of the measured values in each case.

The RMSE and the MARE provide distinct forms of data on the model's predicting ability. The RMSE and MARE are used to determine the model's correctness, and they are defined

$$\text{RMSE} = \sqrt{\frac{1}{n}\sum_{i=1}^{n} [T_i - P_i]^2} \quad (9)$$

$$\text{MARE} = \frac{1}{n}\sum_{i=1}^{n} \left|\frac{T_i - P_i}{T_i}\right| \times 100 \quad (10)$$

in which $n$ denotes the number of data set and $T_i$ and $P_i$ are the measured and predicted values of the chosen property for each case.

as:

Tables 5, 6 and 7 provide the statistical parameter results for the ANN and FL models, as well as for each analyzed property.

Both the ANN and FL models are quite close to the experimental data, as seen in Figures 11, 12 and 13. With a significant determination coefficient (R2) that is close to the unit, the linear least square line fits the points adequately. Furthermore, the ANN and FL outcomes are fairly similar; there is only a small difference. The close R2 and d values found in the cases of ANN and FL support this conclusion. Furthermore, the statistical data shown in Tables 5, 6, and 7 show that in 50% of situations, the model gives the best results and the FL model gives the best results in the other 50 % of case

**Table 5** Tensile strength statistical parameters of proposed ANN and FL models

| Statistical parameters | ANN | | FL | |
|---|---|---|---|---|
| | 80 °C | 120 °C | 80 °C | 120 °C |
| $R^2$ | 0.9273 | 0.9982 | 0.9302 | 0.9718 |
| $d$ | 0.9771 | 0.9986 | 0.9655 | 0.9875 |
| RMSE | 0.3364 | 0.2894 | 0.4472 | 0.8298 |
| MARE | 0.9371 | 1.4821 | 1.8931 | 4.9634 |

**Table 6** Elongation at rupture statistical parameters of proposed ANN and FL models

| Statistical parameters | ANN | | FL | |
|---|---|---|---|---|
| | 80 °C | 120 °C | 80 °C | 120 °C |
| $R^2$ | 0.9163 | 0.9957 | 0.8438 | 0.9528 |
| $d$ | 0.9329 | 0.9987 | 0.9371 | 0.9843 |
| RMSE | 22.2756 | 7.9608 | 15.9634 | 27.0543 |
| MARE | 2.8412 | 1.4287 | 1.8785 | 4.7918 |

**Table 7** Hot Set Test statistical parameters of proposed ANN and FL models

| Statistical parameters | ANN | | FL | |
|---|---|---|---|---|
| | 80 °C | 120 °C | 80 °C | 120 °C |
| $R^2$ | 0.9810 | 0.9673 | 0.9897 | 0.9883 |
| $d$ | 0.9878 | 0.9909 | 0.9956 | 0.9959 |
| RMSE | 3.9625 | 5.7491 | 2.1677 | 3.8367 |
| MARE | 1.9963 | 2.2483 | 1.5573 | 2.6777 |

Considering the determination coefficient ($R^2$), ANN model gives the best results in three cases which are: prediction of tensile strength at 120 $^0$C and prediction of elongation at rupture at 80 and 120 $^0$C.This model represents in these cases 2.72, 8.59 and 4.5 % as improvements over FL model. However, the FL model gives best performances of prediction as for the remaining cases.FL model has an improvement of 0.31 % in the case of tensile strength prediction at 80 $^0$C over ANN model. In the case of Hot Set test prediction at 80 and 120 $^0$C, it represents improvements of 0.89 and 2.17 %, respectively. In terms of agreement index d, the obtained results are consistent with $R^2$ and show that the two models seem to have the same quality of prediction. From this point of view, ANN model is better than FL model in the following cases: prediction of tensile strength at 80 and 120 $^0$C and prediction of elongation at rupture at 120 $^0$C.In all these cases, ANN model has improvements of 1.2,1.12 and 1.46 %respectively.

On the other hand, FL model gives the best results in the following cases: prediction of elongation at rupture at 80 $^0$C and prediction of Hot

Set Test at 80 and 120 $^0$C.In a quantitative way, FL model represents here improvements of0.45, 0.79 and 0.5 % for different cases, respectively. Furthermore, the computed root mean square error (RMSE) results follow the same trend as the agreement index d. The ANN model is also shown in Tables 5, 6, and 7, the best quality of prediction in three cases which are: prediction of tensile strength at 80 and 120 $^0$C and prediction of elongation at rupture at 120 $^0$C.In these cases, ANN model has respectively 24.78, 65.12 and 70.57 % improvements over FL model. Indeed, FL model has the best quality of prediction in the rest of cases, namely prediction of elongation at rupture at 80 $^0$C and prediction of Hot Set Test at 80 and 120 $^0$C.In these cases, FL model has improvements over ANN model of 28.34,45.29 and 33.26 % respectively. Tables 5, 6, and 7 show that in the majority of cases, the ANN model outperforms the FL model in terms of mean absolute relative error (MARE).ANN model has superior performances in 66.66 % of cases versus 33.33 % of cases for FL model. The ANN model achieved 50.5, 70.14, 70.18 and 16 % improvements over FL in the cases of tensile strength prediction at 80 $^0$C and 120 $^0$C, elongation at rupture prediction at 120 $^0$C and Hot Set Test prediction at 120 $^0$C, respectively, while FL model achieved 33.88 and 22 % improvements over ANN model in the cases of elongation at rupture prediction at 80 $^0$C and Hot Set Test prediction at 80 $^0$C respectively.

In order to evaluate more the relative performances of ANN and FL models, Bland-Altman plots are illustrated in Figs.14a,b,15a,b and 16 a,b. Bland –Altman plot is very simple to do and interpret. It is thought to be a viable alternative to correlation and regression analysis. The X-axis depicts the property's mean values, while the Y-axis depicts the difference between the measured and forecasted values. The Bland–Altman plots, based on all of these figures, are likewise consistent with previous findings. It is visible in Fig.14a,b that variation between measured and both ANN and FL predicted values of tensile strength is within $\pm$ 1 N/mm$^2$ at 80 $^0$C and $\pm$

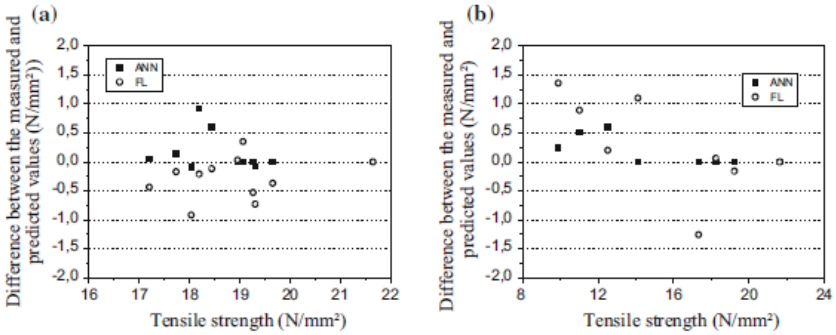


**Fig. 14** Bland–Altman plot of tensile strength: a 80 °C and b 120 °C

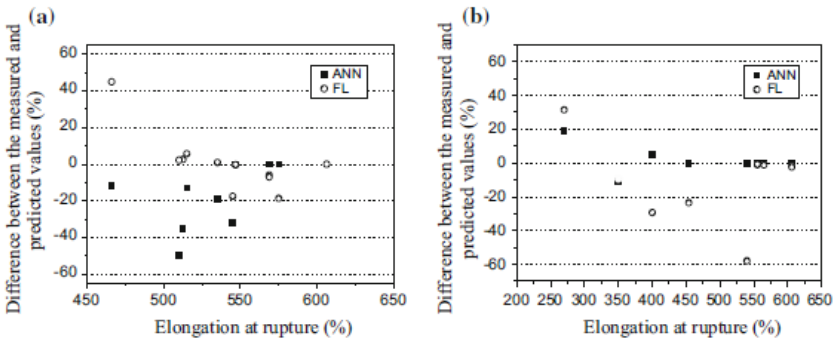


**Fig. 15** Bland–Altman plot of elongation at rupture: a 80 °C and b 120 °C

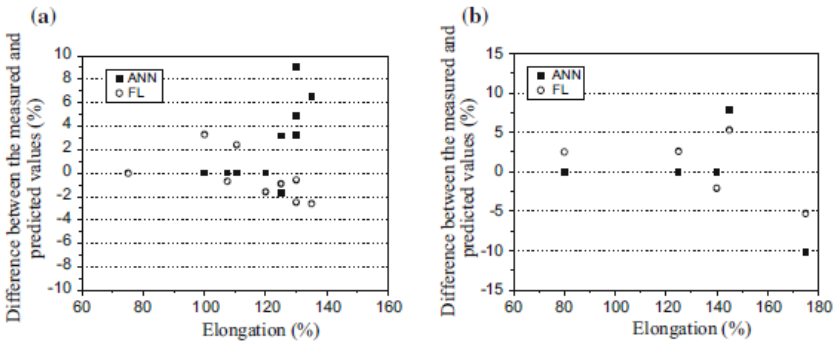


**Fig. 16** Bland–Altman plot of Hot Set Test: a 80 °C and b 120 °C

1.5 N/mm$^2$ AT 120 $^0$C.This result is in good agreement with the small findings of RMSE and MARE in these cases (Table 5).So both models can predict tensile strength with a greater accuracy and prove to be best techniques for modeling and prediction. For elongation at rupture, the Bland-Altman plot (Fig. 15a, b) reveals that the error values of prediction by both ANN and FL models are $\pm$ 50 % for aging temperature 80 $^0$C and vary between -60 and + 30 % for aging temperature 120 $^0$C.This large dispersion of values explains well the big values of RMSE and MARE illustrated in Table 6.From Bland-Altman plot in Fig. 16a, b, it is observed that measured and predicted values of Hot Set Test present about $\pm$ 10 % difference. This result is similar to the ones shown in Table 7.

## V. CONCLUSION

This study looked into using neural networks and fuzzy logic to forecast accelerated thermal ageing of cross-linked polyethylene characteristics. Mechanical properties, which are a good predictor of XLPE thermal deterioration, deteriorate with ageing time, according to the experimental data. The main cause of the loss of mechanical characteristics is the chain session and oxidation process. The degradation of the XLPE was emphasized by an increase in the material's cross-linking degree (higher Hot Set Test).

The use of neural networks and fuzzy logic models to predict the properties of XLPE under thermal ageing provides an alternative to laboratory tests that need specialized materials and knowledge. The suggested ANN and FL models accurately duplicate the same nonlinear features discovered in the lab,

with acceptable error, and provide values that are extremely close to the experimental results. The use of ANN is motivated by its ability to learn from experimental sets, while the use of FL is motivated by its reasoning power.

In this work, we found that both ANN and FL models have nearly identical performance and can accurately predict insulation behavior during thermal ageing.

Using the developed ANN and FL models to predict the mechanical properties of the insulations for ageing times not reached experimentally (generalization phase) to establish the lifetime of the materials and their temperature indexes is suggested as a form of future work, taking into account the results of our investigations. Our future research on intelligent prediction systems will include the creation of a combination neuro-fuzzy methodology.

## REFERENCES

[1]. Ilie S, Setnescu R, Lungulescu EM, Marinescu V, Ilie D, Set- nescu T, Mares G (2011) Investigations of a mechanically failed cable insulation used in indoor conditions. Polym Test 30:173–182

[2]. http://www.nationalgrid.com/NR/rdonlyres/C9AF5612-DF25- 4FCF-ABB5-69F237ACB0C5/3411/SPTTS25.pdf. Accessed 11 May 2014

[3]. Yamanaka T, Maruyama S, Tanaka T (2003) The development of DC ± 500 kV XLPE cable in consideration of the space charge accumulation. In: IEEE 7th international conference on properties and applications of dielectric materials (ICPADM), Nagoya, Japan, pp 689–694

[4]. Dissado LA, Fothergill JH (1992) Electrical degradation and breakdown in polymers. Peter Peregrinus Ltd, London

[5]. Plopeanu M, Notingher PV, Stancu C, Grigorescu S (2011) Elec trical ageing of polyethylene power cables insulation subjected to an electric field in the presence of water. In: 7th international sympo sium on advanced topics in electrical engineering, Bucharest, pp 1–4

[6]. Reich L, Stivala SA (1971) Elements of polymer degradation. McGraw-Hill, New York

[7]. Struik LCE (1978) Physical aging in amorphous polymers and other materials. Elsevier Press, Amsterdam

[8]. Boukezzi L, Boubakeur A, Laurent C, Lallouani M (2007) DSC study of artificial thermal aging of XLPE insulation cables. In: 9th IEEE international conference on solid dielectrics (ICSD), pp 146–149, Winchester, UK, July 8–13 2007

[9]. Mecheri Y, Boukezzi L, Boubakeur A, Lallouani M (2000) Dielectric and mechanical behaviour of cross-linked polyethylene

[10]. under thermal aging. In IEEE annual report, conference on electrical insulation dielectric phenomena (CEIDP), pp 560–563

[11]. Boukezzi L, Nedjar M, Mokhnache L, Lallouani M, Boubakeur A (2006) Thermal aging of cross-linked polyethylene. Ann Chimie Sci Matériaux 31(5):561–569

[12]. Xu Y, Luo P, Xu M, Sun T (2014) Investigation on insulation material morphological structure of 110 and 220 kV XLPE retired cables for reusing. IEEE Trans Dielectr Electr Insul 21(4):1687–1696

[13]. Xie A, Zheng X, Li S, Chen G (2009) The conduction characteristics of electrical trees in XLPE cable insulation. J Appl Polym Sci 114:3325–3330

[14]. Bao M, Yin X, He J (2011) Analysis of electrical tree propagation in XLPE power cable insulation. Phys B 406(8):1556–1560

[15]. Li J, Zhao X, Yin G, Li S (2011) The effect of accelerated water tree ageing on the properties of XLPE cable insulation. IEEE Trans Dielectr Electr Insul 18(5):1562–1569

[16]. Abderrazzaq MH (2012) The impact of electrical treeing on a cable-embedded fibre. Electr Power Syst Res 86:28–33

[17]. Choo W, Chen G, Swingler SG (2011) Electric field in polymeric cable due to space charge accumulation under DC and temperature gradient. IEEE Trans Dielectr Electr Insul 18(2):596–606

[18]. Hussin N, Chen G (2012) Analysis of space charge formation in LDPE in the presence of crosslinking byproducts. IEEE Trans Dielectr Electr Insul 19(1):126–133

[19]. Gulmine JV, Janissek PR, Heise HM, Akcelrud L (2003) Degradation profile of polyethylene after artificial accelerated weathering. Polym Degrad Stab 79:385–397

[20]. Tavares AC, Gulmine JV, Lepienski CM, Akcelrud L (2003) The effect of accelerated aging on the surface mechanical propertiesof polyethylene. Polym Degrad Stab 81:367–373

[21]. Fothergill JC, Dodd SJ, Dissado LA (2011) The measurement of very low conductivity and dielectric loss in XLPE cables: a possible method to detect degradation due to thermal aging. IEEE Trans Dielectr Electr Insul 18(5):1545–1553

[22]. Diego JA, Belana J, Orrit J, Cañadas JC, Mudarra M (2011) Annealing effect on the conductivity of XLPE insulation in power cable. IEEE Trans Dielectr Electr Insul 18(5):1555–1561
[23]. Sadrmomtazi A, Sobhani J, Mirgozar MA (2013) Modeling compressive strength of EPS lightweight concrete using regression, neural network and ANFIS. Constr Build Mater 42:205–216
[24]. Özger M (2011) Prediction of ocean wave energy from meteorological variables by fuzzy logic modelling. Expert Syst Appl 38:6269–6274
[25]. Benli H (2013) Determination of thermal performance calculation of two different types solar air collectors with the use of artificial neural networks. Int J Heat Mass Transf 60:1–7
[26]. Kuşan H, Aytekin O, Özdemir I (2010) The use of fuzzy logic in predicting house selling price. Expert Syst Appl 37:1808–1813
[27]. Chen HC, Gu FC, Wang MH (2012) A novel extension neural network based partial discharge pattern recognition method for high-voltage power apparatus. Expert Syst Appl 39:3423–3431
[28]. Mohanty S, Ghosh S (2014) Breakdown voltage of solid insulations: its modeling using soft computing techniques and its microscopic study. Electr Power Energy Syst 62:825–835
[29]. Teguar M, Mekhaldi A, Boubakeur A (2012) Prediction of polluted insulators characteristics using artificial neural networks. In: IEEE, annual report conference on electrical insulation and dielectric phenomena (CEIDP), pp 767–770
[30]. Gençoğlu MT, Cebeci M (2009) Investigation of pollution flashover on high voltage insulators using artificial neural net-work. Expert Syst Appl 36:7338–7345
[31]. El-Hag AH, Jahromi AN, Pasand MS (2008)
[32]. Prediction of leakage current of non-ceramic insulators in early aging period. Electr Power Syst Res 78:1686–1692

Kodathalapalli Sudheer, et. al. "To predict mechanical properties of XLPE insulation cables under thermal ageing using neural networks and fuzzy logic techniques." *International Journal of Engineering Research and Applications (IJERA)*, vol.12 (03), 2022, pp 05-19.